Int. J. Electrochem. Sci., 10 **(2015)** 1563 - 1573

International Journal of
ELECTROCHEMICAL
SCIENCE
www.electrochemsci.org

Short Communication

A New Method for Preparation of TiO_2 Nanowire Array-Based Photoanodes for Stable Dye-Sensitized Solar Cells

Ming La[*], *Yunxiao Feng, Changdong Chen, Chengye Yang, Songtian Li*

College of Chemistry and Chemical Engineering, Pingdingshan University, Pingdingshan, Henan 467000, People's Republic of China
[*]E-mail: mingla2011@163.com

Received: 4 November 2014 / *Accepted:* 15 November 2014 / *Published:* 30 December 2014

We report the improvement of the open-air stability of photoanode in dye-sensitized solar cells (DSSCs) by treating the TiO_2 nanowire array with silanization agent. The spatially accessible structure of the ordered one-dimensional TiO_2 nanowire array facilitates the uniform polymerization of trichloromethylsilane. The formation of polysiloxane on the surface of N3-sensitized TiO_2 nanowire was verified by Fourier Transform infrared spectroscopy (FTIR) and energy-dispersive spectrometry (EDS) tests. The reaction time for silanization treatment was optimized to be 10 min. The formed polysiloxane can act as a capping layer to prevent the detachment of dye molecules from the surface of TiO_2 nanowires. Current density-voltage (J-V) results displayed that silanization treatment can significantly improve the stability of the TiO_2 nanowire array-based photoanode. No significant loss in cell efficiency was observed after the silane treated photoanode being exposed in air for 30 days.

Keywords: Dye-sensitized solar cells, TiO_2 nanowire, surface modification, stability

1. INTRODUCTION

Due to the rapid depletion of fossil fuels and the escalation in environmental pollution, there is an urgent need for exploring clean and renewable sources to fulfill the ever-increasing energy demand from human society. Photovoltaic (PV) cells are considered one of the most important renewable power sources. Driven by advances in technology, power conversion efficiencies of about 25% have been reached for Si single crystal based PV cells and of 41% for multijunction GaInP/GaInAs/Ge based cells [1]. However, the performance of these cells is still lower than the predicted values. Moreover, they make use of expensive materials and employ complicated and costly processing steps. Due to their low cost and facile fabrication, dye-sensitized solar cells (DSSCs) have been widely explored as a promising alternative to conventional solar cells [2].

One of the most successful DSSC configurations is the Grätzel cell [3], in which the photoanode is a fluorine-doped tin oxide coated glass (glass/FTO) transparent conductor that is coated with a mesoporous TiO_2 semiconductor film, which is sensitized with a Ru bipyridyl dye containing carboxylic acid/carboxylate groups for binding (usually N719 or N3). The counter electrode is a Pt film on glass/FTO, and the electrolyte consists of an I^-/I_3^- redox couple dissolved in organic solvent, such as acetonitrile. Optimized DSSCs have reached a considerable solar-to-electrical power conversion efficiency of 12.3% at AM 1.5G [4]. This efficiency, while currently limited to laboratory prototypes, is promising when compared to the 13–25% efficiency observed for Si PV cells, thus opening the opportunity to effectively exploit the DSSC technology. In an attempt to improve the solar cell performance, many studies have focused on the development of new dyes, nanostructured semiconductor electrodes, and the electrolytic solution [2]. However, apart from the requirement of high device efficiency, the long-term stability of DSSC operation is also a key aspect in terms of practical applications [5-8].

The TiO_2/dye interface is critically important for good long-term DSSC stability [9-11]. Previous studies demonstrated excellent stability for two sealed DSSC cells that were irradiated continuously for 7000 h at one sun illumination, even when raising the temperature to 75 °C for 700 h [12]. Although these results are promising, there are conditions when DSSC stability is a major issue, and several publications express serious concern about the long-term stability for 15−20 years [13, 14]. There are many potential stability issues, but degradation [7, 13] and desorption [15, 16] of dye are among the biggest concerns. It is well-known that Ru-based dye is not stable in air when adsorbed to TiO_2, especially if water is present, making it necessary to seal the cell immediately [17, 18]. Poor air and water stability can be issues in the processing of DSSCs. To dealing with problem, two different strategies have been proposed for improving the stability of dyes on the TiO_2/dye interface: i) using dyes with special anchoring groups [16, 19, 20]; ii) covalent bonding of dyes to metal oxide surfaces [15, 21]. The most common interaction between dyes with TiO_2 reported is through the carboxylate/carboxylic acid group ($COOH/COO^-$) [22]. The attachment is usually described as a combination of bidentate bridging and hydrogen bonding modes [23, 24]. The phosphonate group has also been widely used for the adsorption of various sensitizers because it binds more strongly and with greater stability compared to $COOH/COO^-$ [24-26]. Recently, phosphoric acid has been employed as the anchoring group in various dyes and has showed superiority over carboxylic acid for improving the long-term stability of the cells [16, 25, 27]. Covalent bonding of dye to TiO_2 surface is another attachment strategy to impede the dissolution of the dye into the electrolyte. The most common occurs by either of dye molecules and direct attachment to the metal oxide or silanization of the metal oxide followed by attachment of the dye through organic coupling, such as amide bond formation [28-30].

However, both of the above-mentioned strategies require the alteration of the dye molecules, which often involve intricate synthesis processes and even deteriorate the performance of the dyes such as lowering the electron injection efficiency and light absorption ability. Herein, we reported a novel method for improving the long-term stability of the TiO_2/dye interface by employing polysiloxane as the caging layer for immobilizing the adsorbed dyes. This method can be applied after the adsorption of dyes onto the TiO_2 surface and without structural modification of the dyes molecules.

Trichloromethylsilane as a silanization agent for passivating the surface of TiO_2 nanoparticles was firstly proposed by Gregg et al. to inhibit the interfacial recombination between the injected electrons in the TiO_2 (e_{TiO2}) with the oxidized species of the redox couple (normally I_3^-) [31]. However, in this case, the nanoparticle-shaped TiO_2 was used as the basic material for the adsorption of dye and the treatment of the trichloromethylsilane. Within this nanopartical-piled structure, the pores in the TiO_2 film were tending to be plugged during the silanization procedure. Furthermore, this structure prevents the homogeneous diffusion of silane gas to the surface of the TiO_2 to form uniform passivation layer [31, 32]. It is noticeable that the use of silane-coated one-dimensional TiO_2 nanowire arrays for DSSCs could mitigate this problem. The open and spatially accessible structure of the TiO_2 nanowire array is favorable for the coating of uniform polysiloxane layer.

Thus, in this study, we employed the one dimensional TiO_2 nanowires instead of nanoparticle-baed TiO_2 for supporting dyes. The open-structured nanowire TiO_2 film could provide a direct pathway for the diffusion of the silane reagents which facilitate the formation of uniform capping layer. In addition, the phase continuation in TiO_2 nanowires is propitious for the transportation of injected electrons [33, 34]. Silanization treatment of the dye-adsorbed TiO_2 nanowire arrays would lead to the formation of a thin capping layer which could prevent the detachment of dyes from the surface of TiO_2 nanowire array. The results showed that the capping protection strategy dramatically improves the stability under variety of conditions important for DSSC operation and processing with very little decrease in the efficiency.

2. EXPERIMENTAL

2.1 Chemicals and reagents

Cis-bis-(isothiocyanato) bis(2,2′-bipyridyl-4,4′-dicarboxylato) ruthenium(II) bis-tetrabutylammonium (N3) was purchased from Solaronix (Switzerland). Transparent conductive glass (F-doped SnO2, FTO, 15 Ω/square, transmittance of 80%) was received from Nippon Sheet Glass Company (Japan). Other chemicals were used as received from commercial sources without further purification.

2.2 Preparation of the TiO_2 nanowire arrays

The TiO_2 nanowire arrays were directly grown on FTO substrates using a modified reported method [35]. In a typical synthesis, 1 mL of hydrochloric acid (37 wt %) was mixed with 10 mL of toluene, then 1 mL of tetrabutyl titanate was added. The mixture was stirred for 5 min and 1mL of titanium tetrachloride (1 M intoluene) was added, the final mixture was poured in a Teflon reactor.

The FTO substrates, cleaned by sonication in acetone, 2-propanol, and ethanol, subsequently rinsed with deionized (DI) water, and dried in a nitrogen stream. Before the grown of nanowire arrays, the well-cleaned FTO substrate was coated with a compact TiO_2 layer by treating the substrate with a 0.2 M $TiCl_4$ aqueous solution for 12 h, and subsequent annealing in air at 500 °C for 0.5 h. The as-treated FTO substrate was placed in the Teflon reactor containing the precursor solution. The hydrothermal synthesis was conducted at 180 ^oC for 4 h in an electric oven. After synthesis, the autoclave was cooled to room temperature under flowing water. The FTO substrate was taken out, rinsed extensively with ethanol, and deionized water. Subsequently the films were sintered in a furnace at 450 ^oC for 30 min. Hot TiO_2 nanowire films were immersed in a dye bath containing 0.5 mM N3 in ethanol overnight. The films were then rinsed in ethanol to remove excess dyes.

2.3 Silanization treatment of the dye-absorbed TiO_2 nanowire arrays

The vapor-phase silanization procedure was carried out on a home-made chamber equipped with inlet and outlet valves by referring reported methods [31, 32]. Firstly, the chamber was loaded with N3-sensitized TiO_2 nanowire and flushed with N_2 gas for 30 min. Trichloromethylsilane (0.5 mL) was then introduced through a long glass pipe into a small container. After keeping the silanization reaction for a certain time, the TiO_2 nanowire films were taken out and rinsed with acetonitrile (containing 2% pyridine, v/v) and baked at 100 ^oC for 15 min.

2.4 DSSC fabrication and photovoltaic measurements

The silane treated N3-sensitized TiO_2 nanowire substrate was used as the photoanode, and a platinum-coated FTO glass was used as the counter electrode. The photoanode and Pt counter electrode were assembled into a sandwich-type cell and sealed with a 25 μm thick Surlyn 1702 (Dupont) gasket. A drop of the electrolyte, a solution of 0.05 M I_2, 1 M MPII, 0.5 M guanidine thiocyanate, and 0.5 M *tert*-buthylpyridine in acetonitrile, was deposited through the hole in the back of the counter electrode. The electrolyte was introduced into the cell via capillary action. Then, the hole was sealed using the same Surlyn film and a cover glass (0.7 mm thick).

The current density-voltage (J-V) characteristics of the DSSCs were measured using a Keithley 2400 source meter under the illumination of AM1.5G simulated solar light (Oriel-91193 equipped with a 1000 W Xe lamp and an AM1.5 filter). The solar energy-to-electricity conversion efficiency was calculated with eq 1 [2].

$$\eta = \frac{J_{sc} \times V_{oc} \times FF}{P_{oc}} \qquad (1)$$

Where η is overall solar-to-electrical energy conversion efficiency, J_{sc} is the photocurrent density measured at short-circuit, V_{oc} is the open–circuit photovoltage, FF is the fill factor of the cell, and P_{in} is the intensity of the incident light.

3. RESULTS AND DISCUSSION

3.1 Characterization of TiO_2 nanowire arrays

The morphology of the TiO_2 nanowire array was characterized by scanning electron microscope (SEM). Figure 1 shows the top views and cross-sectional images of a typical synthesized nanowire film. The TiO_2 array consisting of vertically aligned and cylinder shaped nanowires which have small feature sizes (an average diameter of ∼40 nm and a typical length of ∼4 μm). The hydrothermal growth of vertically oriented TiO_2 nanowire arrays on FTO with feature sizes of ∼20 nm via a nonpolar solvent/hydrophilic solid substrate interfacial reaction was first reported by Grimes and co-workers [35], and this method has been successfully used to synthesize TiO_2 nanowires in some other cases [33, 36, 37]. In this hydrothermal system, hydrochloric acid is used to ensure an acidic environment and retard hydrolysis of the precursor in the presence of water. Meanwhile, the Cl^- ions play an important role in the hydrothermal growth as they promote anisotropic growth of one-dimensional nanocrystals. The Cl^- ions are inclined to absorb on the rutile (110) plane, thus retarding further growth of this plane [34, 35].

The dye loading measurement was conducted by redissolving dye molecules which adsorbed on the TiO_2 nanowire array into 1M NaOH solution and then measuring the absorbance of the resultant solution. The calculated dye loading amounts for the TiO_2 nanowire film was 28.4 nmol/cm^2. Using a dye adsorption area of 1.6 nm, a roughness factor of ~277 for the TiO_2 nanowire film was obtained. This value is inferior to that of the conventional nanoparticles-based structure. But it is comparable to that measured from other one-dimensional structured-TiO_2 films [34, 35].

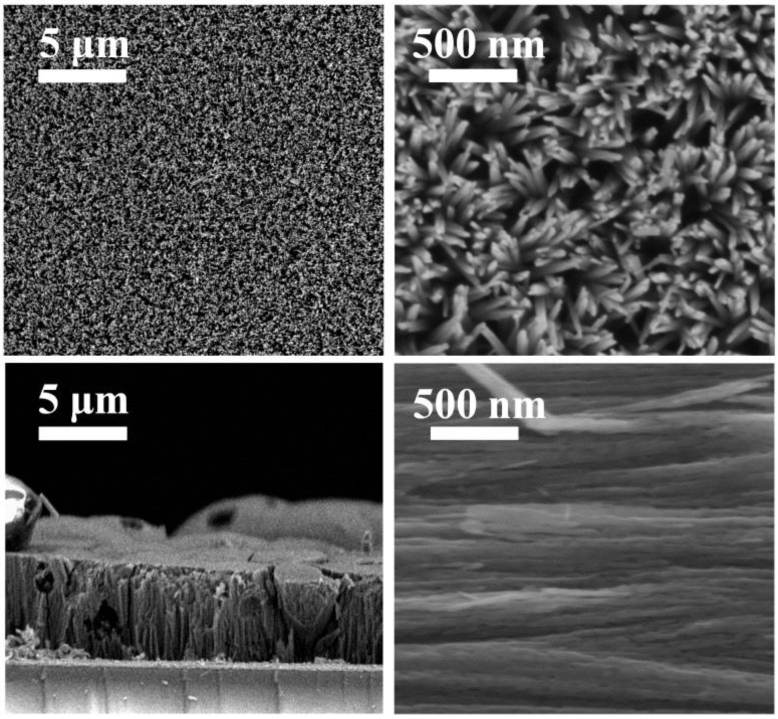

Figure 1. SEM images of TiO_2 nanowire arrays grown on FTO in top- (panels A and B) and cross-sectional (panels C and D) views.

3.2 Silanization treatment of the dye-absorbed TiO_2 nanowire arrays

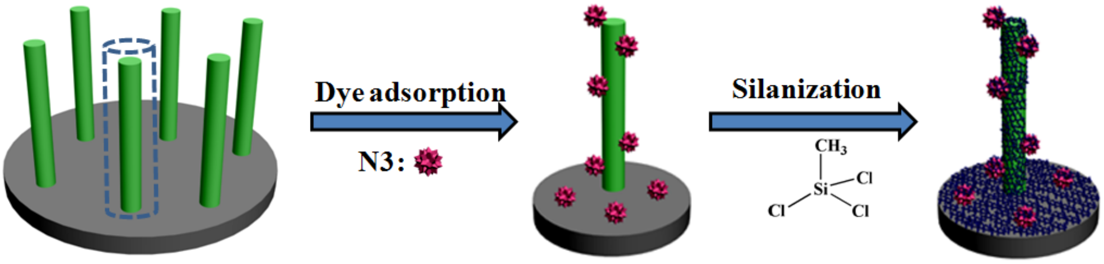

Figure 2. Schematic illustrating silanization treatment of the dye-absorbed TiO_2 nanowire array.

It is clear that further improvements in DSSC stability is still needed to realize commercial applications in the future. Here we employ polysiloxane as a capping layer to fix the dye molecules and impede the dissolution of the dye into the electrolyte. The silanization procedure was depicted in Figure 2. The TiO_2 nanowire array was firstly treated with N3 dye solution, and then the obtained N3-sensitized TiO_2 nanowire was covered with a thin layer of polysiloxane which was polymerized from trichloromethylsilane. This method has successfully been conducted for the treatment of the TiO_2 surfaces [31, 32]. The reaction of silanes with silica has extensively studies by Hair's group [38, 39]. Similar to that, trichloromethylsilane can react quickly and irreversibly with hydroxyl groups on the surface of the TiO_2 nanwires, and in the presence of trace amount of H_2O, the silane molecules can react with each other to form cross-linked polysiloxane layer. Humidity and reaction time are critical factors for manipulate the properties of the polysiloxane layer. Under a relatively low humidity condition (by flushing the reaction chamber with N_2 for 10 min), the thickness of the polysiloxane layer was regulated by adjusting the reaction time. The formation of polysiloxane layer on the surface of N3-sensitized TiO_2 nanowire array was characterized by FTIR and EDS techniques.

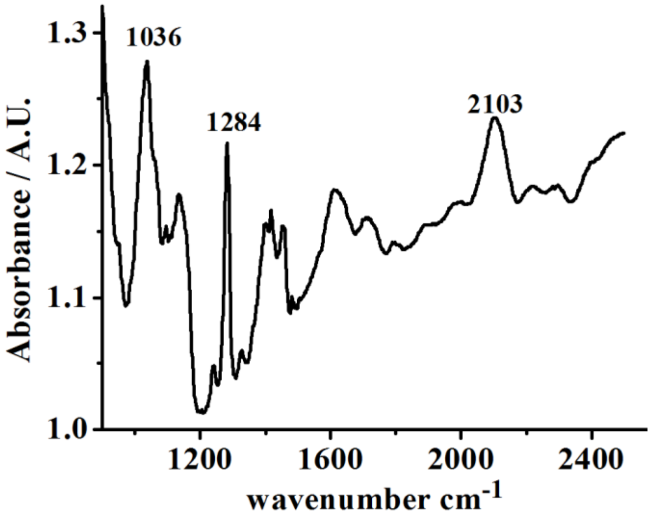

Figure 3. FTIR spectrum of the silanization treated N3-sensitized TiO_2 nanowire array.

Figure 3 shows FTIR spectrum of N3-sensitized TiO_2 after treating with trichloromethylsilane for 5 min. A bond at about 1036 cm^{-1} can be attributed to the Si-O-Si stretching vibration. A characteristic bond at about 1284 cm^{-1} was also observed, which can be ascribed to CH_3 bending [32, 40]. The peak at 2103 cm^{-1} is due to the CN stretch from the two SCN ligands on N3. In order to further understand the element composition of the N3-sensitized TiO_2 nanowire array, the EDS spectra were obtained both before and after the silanization treatment. The results were shown in Figure 4 and table 1. Before the silanization treatment (Figure 4A), characteristic peaks of O, Ru, Ti elements were observed. In comparison, the peak of Si was appeared in the spectrum (Figure 4B) for the sample after silanization treatment. In addition, the percentage of oxygen element dramatically increased (table 1), implying the presence of the polysiloxane. Therefore, the studies of FTIR and EDS indicate that polysiloxane layer has been succesfuly formed on the surface of N3-sensitized TiO_2 nanowire array.

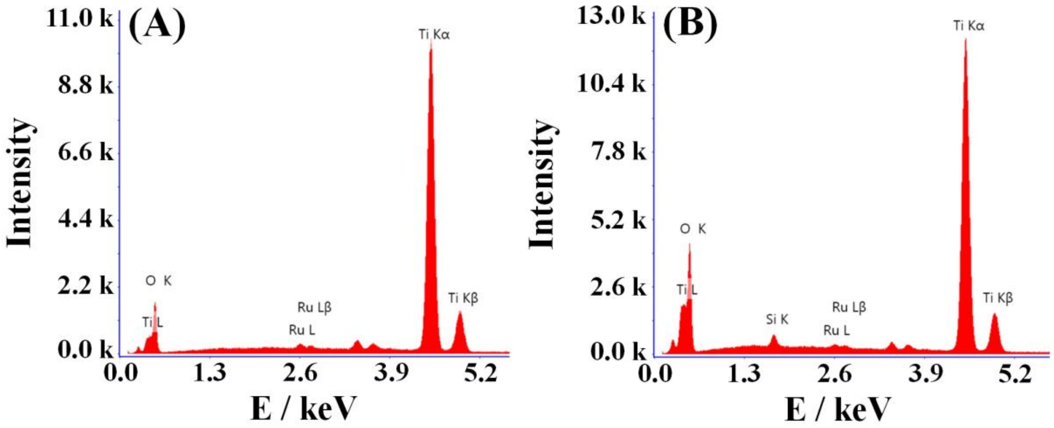

Figure 4. EDS spectra of N3-sensitized TiO_2 nanowire arrays before (A) and after (B) silanization treatment.

Table 1. EDS atoms percentages (i.e., O, Si, Ru, Ti) before and after silanization treatment .

	O (%)	Si (%)	Ru (%)	Ti (%)
Before silanization	40.84	0	0.73	58.43
After silanization	71.31	0.84	0.23	27.62

To avoid the loss of efficiency in the assembled cells, the thickness of the polysiloxane layer for coating N3-sensitized TiO_2 nanowire assay was regulated by adjusting the reaction time. As stated in previous report, long time for trichloromethylsilane treatment would lead to the reduction of photocurrent and corresponding efficiency loss of the cells [31, 32]. Therefore, an optimal thickness of the silanization layer needs to be determined, which can effectively impede desorption of dye molecules while exerts little influence on the electron transfer kinetics between the dye and the redox couple in electrolyte.

Table 2. Parameters for cells based on N3-sensitized TiO_2 nanowire arrays with different silanization treating time.

Treating time (min)	J_{sc} (mA/cm^2)	V_{oc} (Volt)	Fill factor	Efficiency(%)
0	8.73	0.731	0.619	3.95
5	8.55	0.743	0.633	4.02
10	8.31	0.760	0.652	4.12
20	7.39	0.767	0.656	3.72
30	5.64	0.772	0.670	2.92
40	4.21	0.774	0.657	2.14
50	3.13	0.778	0.645	1.57

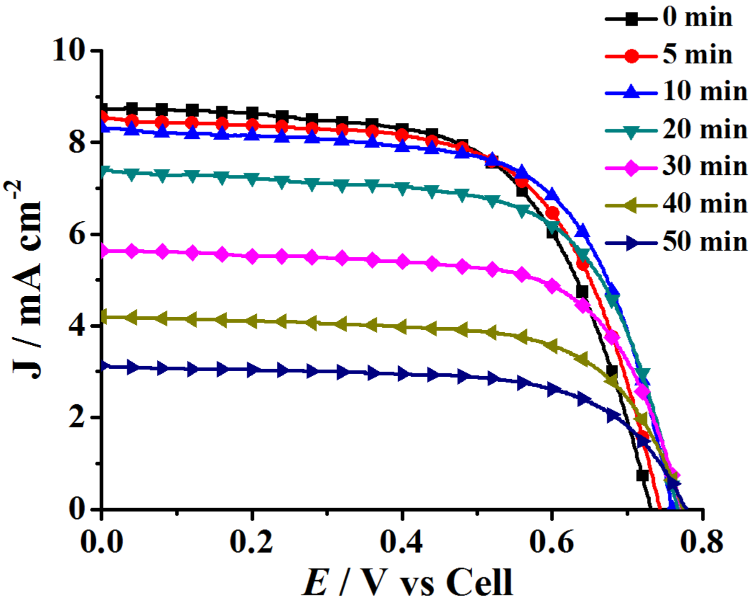

Figure 5. Current density *J* plotted against potential *E* at the N3-sensitized TiO_2 nanowire arrays with different silanization treating time under the illumination of light equivalent to one sun.

The performances of cells fabricated from N3-sensitized TiO_2 nanowire arrays with different silanization treating time are shown in Figure 5 and table 2. The cell based on TiO_2 nanowire array without silanization treatment exhibits a short-circuit current of 8.73 $mA{\cdot}cm^2$, an open-circuit voltage of 0.731 V, and a fill factor of 0.619. The overall power conversion efficiency was found to be 3.95 %. The results show that this nanowire-structured TiO_2 film can be used as a convenient and effective photoanode in the DSSCs. And a higher efficiency could further be achieved by optimizing the structure of the TiO_2, especially by increasing the roughness factor of the TiO_2 nanowire film. And an increase in V_{oc} value was observed while prolonging the silanization treating time. This is probably due to that polysiloxane layer covered on the N3-sensitized TiO_2 nanowire arrays not only colud fix the dye molecules but also inhibit the interfacial recombination between the injected electrons in the TiO_2 with I_3^- in electrolyte. The J_{sc} values declined significantly when the silanization treating time exceeded 20 min, indicating that thick polysiloxane layer could hinder the electron transfer between dyes with the redox couple in solution and lead to the inactive of dye molecules. The cell showed an optimal efficiency of 4.02% with a silanization treating time of 10 min. Therefore in the following studies, the time for treating N3-sensitized TiO_2 nanowire arrays with trichloromethylsilane was fixed at 10 min.

3.3 Stability study

It is known that photoanodes for DSSCs based on ruthenium dyes are not stable indefinitely [14, 15]. Exposure to air, water, UV light, heat, and other chemicals can lead to desorption and degradation of dye molecules over time. To evaluate the capability of polysiloxane layer for improving the stability of the photoanode, we tested the performances of cells based on N3-sensitized TiO_2 nanowire arrays (before and after the silanization treatment) exposure to air for up to 30 days.

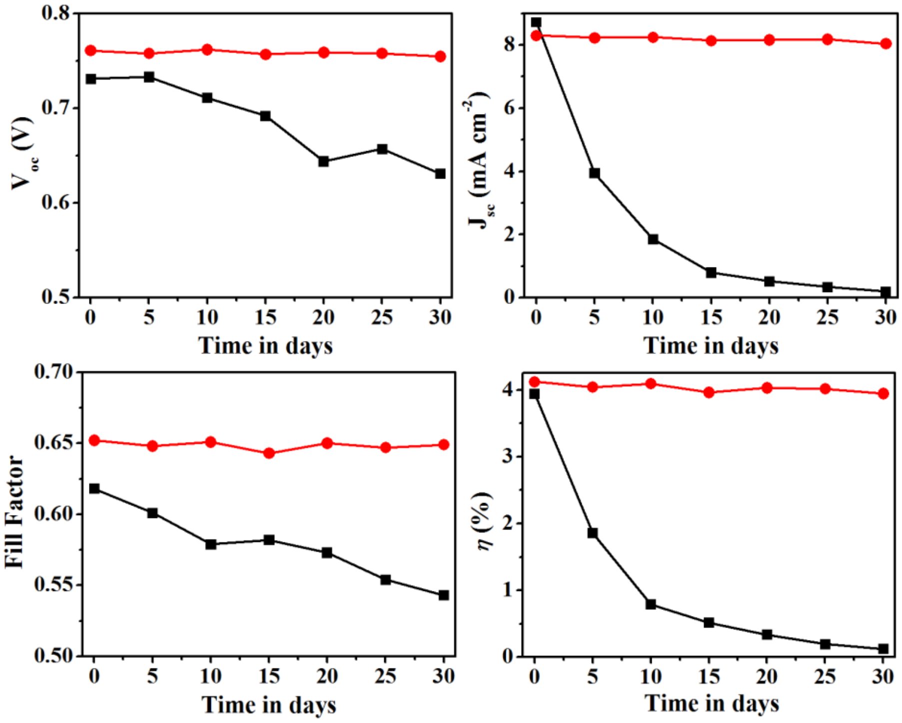

Figure 6. Parameters for cells based on N3-sensitized TiO_2 nanowire arrays with (●) and without (■) silanization treatment.

Figure 6 shows the evolution of *I-V* parameters of cells based on N3-sensitized TiO_2 nanowire arrays with or without silanization treatment. The results indicated that silanization treatment can significantly improve cell performance, mainly by stabilizing the J_{sc}. And no significant loss in cell efficieny was observed for the photoanode which had been exposed in air for 30 days. However, the cell assembled from N3-sensitized TiO_2 nanowire array without silanization treatment showed a significant loss in photoactiviry. Exposure to air for five days leaded to a more that 50% decrease in efficiency. And the cell displayed a complete loss in photoactivity after the photoanode being exposed in air for 25 days, mainly due to the dramatical decrease of J_{sc}. A first hypothesis to explain the improved performance stability of DSSCs utilizing silanization treatment could be the formation of polysiloxane layer on the N3-sensitized TiO_2 nanowire arrays. The ordered structure of TiO_2 nanowire arrays facilitates the uniform polymerization of trimethylchlorosilane. And the formed polysiloxane can act as a capping layer to prevent the detachment of dye molecules from the surface of TiO_2 nanowires.

4. CONCLUSION

In this paper we developed a novel strategy to improve the performance stability of DSSCs by employing TiO_2 nanowire array and silanization treatment. The ordered one-dimensional TiO_2 nanowire array facilitates the uniform polymerization of silane agent. The formation of the polysiloxane layer was comfirmed by FTIR and EDS results. The reaction time was optimized by inspecting operating performance of the corresponding assembled cells. Silanization treatment can significantly improve the stability of the photoanode, mainly by stabilizing the J_{sc}. The formed polysiloxane can act as a capping layer to prevent the detachment of dye molecules from the surface of TiO_2 nanowires. No significant loss in cell efficiency was observed after the photoanode being exposed in air for 30 days.

ACKOWLEDGMENTS
This work was support by the Fund of Department of Science and Technology Department in Henan (KJT142102310462), the Youth Research Foundation in Pingdingshan University (20120015) and the High-Level Personnel Fund in Pingdingshan University (1011014/G).

References

1. M. A. Green, K. Emery, Y. Hishikawa, W. Warta and E. D. Dunlop, *Prog. Photovoltaics*, 2014, 22, 701-710.
2. A. Hagfeldt, G. Boschloo, L. Sun, L. Kloo and H. Pettersson, *Chem. Rev.*, 2010, 110, 6595-6663.
3. B. O'Regan and M. Grätzel, *Nature*, 1991, 353, 737-740.
4. A. Yella, H.-W. Lee, H. N. Tsao, C. Yi, A. K. Chandiran, M. K. Nazeeruddin, E. W.-G. Diau, C.-Y. Yeh, S. M. Zakeeruddin and M. Grätzel, *Science*, 2012, 334, 629-634.
5. H.-L. Lu, T. F. R. Shen, S.-T. Huang, Y.-L. Tung and T. C. K. Yang, *Sol. Energy Mater. Sol. Cells*, 2011, 95, 1624-1629.
6. K. T. Dembele, R. Nechache, L. Nikolova, A. Vomiero, C. Santato, S. Licoccia and F. Rosei, *J. Power Sources*, 2013, 233, 93-97.
7. G. G. Xue, Y. Guo, T. Yu, J. Guan, X. R. Yu, J. Y. Zhang, J. G. Liu and Z. G. Zou, *Int. J. Electrochem. Sci.*, 2012, 7, 1496-1511.
8. J. Dewalque, N. Ngoc Duy, P. Colson, N. Krins, R. Cloots and C. Henrist, *Electrochim. Acta*, 2014, 115, 478-486.
9. M. Grätzel, *C. R. Chim.*, 2006, 9, 578-583.
10. E. Figgemeier and A. Hagfeldt, *Int. J. Photoenergy*, 2004, 6, 127-140.

11. J. Lim, Y. S. Kwon, S.-H. Park, I. Y. Song, J. Choi and T. Park, *Langmuir*, 2011, 27, 14647-14653.
12. O. Kohle, M. Grätzel, A. F. Meyer and T. B. Meyer, *Adv. Mater.*, 1997, 9, 904-906.
13. H. T. Nguyen, H. M. Ta and T. Lund, *Sol. Energy Mater. Sol. Cells*, 2007, 91, 1934-1942.
14. R. Grünwald and H. Tributsch, *J. Phys. Chem. B*, 1997, 101, 2564-2575.
15. T. Luitel and F. P. Zamborini, *Langmuir*, 2013, 29, 13582-13594.
16. T. N. Murakami, E. Yoshida and N. Koumura, *Electrochim. Acta*, 2014, 131, 174–183.
17. O. Kohle, M. Gratzel, A. F. Meyer and T. B. Meyer, *Adv. Mater.*, 1997, 9, 904-906.
18. H. G. Agrell, J. Lindgren and A. Hagfeldt, *Sol. Energy*, 2003, 75, 169-180.
19. S. M. Zakeeruddin, M. K. Nazeeruddin, P. Pechy, F. P. Rotzinger, R. HumphryBaker, K. Kalyanasundaram, M. Gratzel, V. Shklover and T. Haibach, *Inorg. Chem.*, 1997, 36, 5937-5946.
20. H. Zabri, I. Gillaizeau, C. A. Bignozzi, S. Caramori, M.-F. Charlot, J. Cano-Boquera and F. Odobel, *Inorg. Chem.*, 2003, 42, 6655-6666.
21. W. E. Ford and M. A. J. Rodgers, *J. Phys. Chem.*, 1994, 98, 3822-3831.
22. C. Pérez León, L. Kador, B. Peng and M. Thelakkat, *J. Phys. Chem. B*, 2006, 110, 8723-8730.
23. M. K. Nazeeruddin, R. Humphry-Baker, P. Liska and M. Grätzel, *J. Phys. Chem. B*, 2003, 107, 8981-8987.
24. K. Kilså, E. I. Mayo, B. S. Brunschwig, H. B. Gray, N. S. Lewis and J. R. Winkler, *J. Phys. Chem. B*, 2004, 108, 15640-15651.
25. D. G. Brown, P. A. Schauer, J. Borau-Garcia, B. R. Fancy and C. P. Berlinguette, *J. Am. Chem. Soc.*, 2013, 135, 1692-1695.
26. M. R. Norris, J. J. Concepcion, C. R. K. Glasson, Z. Fang, A. M. Lapides, D. L. Ashford, J. L. Templeton and T. J. Meyer, *Inorg. Chem.*, 2013, 52, 12492-12501.
27. H. Park, E. Bae, J.-J. Lee, J. Park and W. Choi, *J. Phys. Chem. B*, 2006, 110, 8740-8749.
28. J. R. Hohman and M. A. Fox, *J. Am. Chem. Soc.*, 1982, 104, 401-404.
29. C. S. Christ, J. Yu, X. Zhao, G. T. R. Palmore and M. S. Wrighton, *Inorg. Chem.*, 1992, 31, 4439-4440.
30. R. Dabestani, A. J. Bard, A. Campion, M. A. Fox, T. E. Mallouk, S. E. Webber and J. M. White, *J. Phys. Chem.*, 1988, 92, 1872-1878.
31. B. A. Gregg, F. Pichot, S. Ferrere and C. L. Fields, *J. Phys. Chem. B*, 2001, 105, 1422-1429.
32. S. M. Feldt, U. B. Cappel, E. M. J. Johansson, G. Boschloo and A. Hagfeldt, *J. Phys. Chem. C*, 2010, 114, 10551-10558.
33. X. Feng, K. Shankar, M. Paulose and C. A. Grimes, *Angew. Chem. Int. Ed.*, 2009, 121, 8239-8242.
34. B. Liu and E. S. Aydil, *J. Am. Chem. Soc.*, 2009, 131, 3985-3990.
35. X. Feng, K. Shankar, O. K. Varghese, M. Paulose, T. J. Latempa and C. A. Grimes, *Nano Lett.*, 2008, 8, 3781-3786.
36. S. Hoang, S. Guo, N. T. Hahn, A. J. Bard and C. B. Mullins, *Nano Lett.*, 2012, 12, 26-32.
37. S. Hoang, S. Guo and C. B. Mullins, *J. Phys. Chem. C*, 2012, 116, 23283-23290.
38. C. P. Tripp and M. L. Hair, *J. Phys. Chem.*, 1993, 97, 5693-5698.
39. C. P. Tripp, P. Kazmaier and M. L. Hair, *Langmuir*, 1996, 12, 6407-6409.
40. C. P. Tripp and M. L. Hair, *Langmuir*, 1991, 7, 923-927.